Magnetic susceptibilities, specific heat, and crystal structure of four S = 3/2, three-dimensional antiferromagnets

Magnetic susceptibilities, specific heat, and crystal structure of four $S=3/2$, three-dimensional antiferromagnets

K. E. Merabet, Ramón Burriel,* and Richard L. Carlin
Department of Chemistry, University of Illinois at Chicago, Chicago, Illinois 60680

Peter B. Hitchcock, Kenneth R. Seddon, and Jalal A. Zora
School of Chemistry and Molecular Sciences, University of Sussex, Falmer, Brighton BN1 9QJ, United Kingdom

Cheng Gang and Klaas Kopinga
Department of Physics, Eindhoven University of Technology, 5600 MB Eindhoven, The Netherlands
(Received 17 October 1989)

The zero-field, ac magnetic susceptibilities of single crystals of four $S=\frac{3}{2}$ trigonal salts containing the tris(1,2-diaminoethane)chromium(III) cation, $[Cr(en)_3]^{3+}$, and heat-capacity measurements on one of them, $[Na(OH_2)_6][Cr(en)_3]_2Cl_7$, are reported. The crystal structures of two of them, $[Na(OH_2)_6][Cr(en_3]_2Cl_7$ and $[Na(OH)_2)_6][Cr(en)_3]_2Br_6Cl$, have been determined. They both belong to the trigonal $P\bar{3}cl$ space group, with $a=11.513(2)$, $c=15.566(6)$ Å; $Z=2$; and $a=11.740(5)$, $c=16.008(9)$ Å; $Z=2$, respectively, and contain discrete octahedral hexaquasodium (I) cations. The salt $[K(OH_2)_6][Cr(en)_3]_2Cl_7$ appears to be isomorphous with its sodium analog, and $[Cr(en)_3]Cl_3\cdot 3H_2O$ belongs to the same space group. The magnetic measurements on the four salts extend over the temperature interval 60 mK to 4.2 K, and antiferromagnetic ordering is found in all of them. The zero-field-splitting energy is of the same order of magnitude as the magnetic exchange energy. The susceptibility data have been fitted with the parameters $2D/k_B=-0.091(8)$ K, $g_{\parallel}=1.994$, $g_{\perp}=1.988$, and $zJ/k_B=-0.061(2)$ K for $[Cr(en)_3]Cl_3\cdot 3H_2O$; $2D/k_B=-0.058(8)$ K, $g_{\parallel}=2.01$, $g_{\perp}=2.00$, and $zJ/k_B=-0.068(4)$ K for $[Na(OH_2)_6][Cr(en)_3]_2Cl_7$; $2D/k_B=-0.060(8)$ K, $g_{\parallel}=1.993$, $g_{\perp}=1.951$, and $zJ/k_B=-0.046(4)$ K for $[K(OH_2)_6][Cr(en)_3]_2Cl_7$; and $2D/k_B=+0.064(8)$ K, $g_{\parallel}=2.001$, $g_{\perp}=1.991$, and $zJ/k_B=-0.066(4)$ K for $[Na(OH_2)_6][Cr(en)_3]_2Br_6Cl$, where longitudinal ($\parallel$) and transverse ($\perp$) refer to the unique threefold crystallographic axis. The ordering temperatures are 0.124(5), 0.116(5), 0.093(5), and 0.112(5) K, respectively. The easy axis for the chloride compounds lies parallel to the longitudinal axis, whereas the easy axis for the bromide lies in the transverse plane. Heat-capacity measurements on $[Na(OH_2)_6][Cr(en)_3]_2Cl_7$ confirm that magnetic ordering takes place at 0.112(5) K. The heat-capacity curve and magnetic entropy calculations agree with the three-dimensional character of the ordering of an $S=\frac{3}{2}$, effective bcc magnetic lattice.

I. INTRODUCTION

Very few superexchange-coupled chromium (III) antiferromagnets are known. One reason for this is that the exchange is often so weak that ordering takes place only at very low temperatures. One example is provided by $Cs_2CrCl_5\cdot 4H_2O$,[1] which orders at 185 mK. Recent attempts to raise the ordering temperature to a more accessible region have revolved around the preparation and study of bimetallic compounds such as $[Cr(NH_3)_6][Cr(CN)_6]$.[2] This material orders (ferromagnetically) at 600 mK, which admittedly is not much of an increase.

In continuing our studies on chromium salts, which interest us because they exhibit the intermediate spin value of $S=\frac{3}{2}$, we have prepared single-crystal samples of $[Cr(en)_3]Cl_3\cdot 3H_2O$ (en=1,2 diaminoethane; $NH_2CH_2CH_2NH_2$), $[Na(OH_2)_6][Cr(en)_3]_2Cl_7$, $[K(OH_2)_6][Cr(en)_3]_2Cl_7$, $[K(OH_2)_6][Cr(en)_3]_2Cl_7$, and $[Na(OH_2)_6][Cr(en)_3]_2Br_6Cl$. Salts of the $[Cr(en)_3]^{3+}$ cation have been recognized for a long time,[3] although the double salts reported here are novel, and there has been no previous investigation of their magnetic properties at low temperatures. We use the notation such as $[Na(OH_2)_6]\,[Cr(en)_3]_2Cl_7$, rather than the more common $[Cr(en)_3]Cl_3\cdot 0.5NaCl\cdot 3H_2O$ in order to emphasize that the water is coordinated to the alkali metal ion, as discussed in the following. An earlier report[4] on the susceptibility of a polycrystalline sample of $[Cr(en)_3]Cl_3\cdot 3H_2O$ suggested that the Weiss constant was -4 K, which would be suggestive of strong exchange, but the measurements did not extend below 85 K. Chromium (III) has a $^4A_2$ ground state with an axial crystal-field splitting of $2D/k_B$; the sign of D determines whether the ground state is the $|\pm\frac{1}{2}\rangle$ or $|\pm\frac{3}{2}\rangle$ doublet.

The crystal structure of $[Cr(en)_3]Cl_3\cdot 3H_2O$ has been reported.[5] The system is trigonal with space group $P\bar{3}c1$ with four formula units in the unit cell. The compound is composed of discrete, six coordinate D_3 $[Cr(en)_3]^{3+}$ cations and chloride ions linked by hydrogen bonds. There

are four such cations per unit cell, and each one has its trigonal axis parallel to the hexagonal c axis of the unit cell. The waters of hydration are also linked to each other by hydrogen bonds, but no bonds exist between the complexes and the water molecules. The water molecules are located in channels parallel to the c axis at random sites. They create a randomly varying electric field over the $[Cr(en)_3]^{3+}$ ions. It has been found from the electron paramagnetic resonance (EPR) spectra[5] that this field gives rise to a zero-field splitting that varies in magnitude and in the orientation of its principal axes. The amount of water of hydration is variable and the crystal can be completely dehydrated at 120 °C with no change in the unit cell. The crystal structure of $[K(OH_2)_6][Cr(en)_3]_2Cl_7$ does not appear to have previously been reported, but single crystals appear to be similar in habit to the previous sample and the powder diffractogram indicates it to be isomorphous. The water content also appears to be variable. We report here the crystal structures of $[Na(OH_2)_6][Cr(en)_3]_2Cl_7$ and $[Na(OH_2)_6][Cr(en)_3]_2Br_6Cl$.

An EPR investigation[6] of $[Cr(en)_3]Cl_3\cdot 3H_2O$, diluted by the diamagnetic cobalt analog, yielded the following results, the isotropic g value is 1.9900(4) and $|D|=0.036$ cm^{-1}, that is, $|2D/k_B|=0.1$ K. The rhombic E term is zero, as anticipated for the threefold point symmetry of the chromium positions. We present magnetic-susceptibility data for $[Cr(en)_3]Cl_3\cdot 3H_2O$ and $[Na(OH_2)_6][Cr(en)_3]_2Br_6Cl$ on the parallel and perpendicular direction to the trigonal axis from 60 mK to 4.2 K. In the other two compounds, $[Na(OH_2)_6][Cr(en)_3]_2Cl_7$ and $[K(OH_2)_6][Cr(en)_3]_2Cl_7$ the measurements below 1 K have been pursued only in the parallel direction. Each of the compounds has a small zero-field splitting which is comparable in magnitude to the exchange interaction. The compounds are three-dimensional, $S=\frac{3}{2}$ antiferromagnets. The heat capacity of $[Na(OH_2)_6][Cr(en)_3]_2Cl_7$ confirms the existence of the magnetic transition.

II. EXPERIMENTAL

A. Synthesis

The sample of $[Cr(en)_3]Cl_3\cdot 3H_2O$ was prepared according to the established literature method.[7] Single crystals were obtained by evaporation of an aqueous solution containing a few drops of hydrochloric acid. Chemical analyses (Found: C, 18.02%; H, 7.80%; N, 21.25%; Cl, 27.28%. Calculation for $C_6H_{30}Cl_3CrN_6O_3$: C, 18.3%, H, 7.7%; N, 21.4%; Cl, 27.1%).

$[Na(OH_2)_6][Cr(en)_3]_2Cl_7$ was prepared as follows: Solid sodium chloride in a 6:1 (Na:Cr) molar ratio was added to a solution of tris(1,2 diaminoethane)chromium(III) chloride trihydrate in water at 60 °C. Upon cooling, orange crystals of the product separated from solution, which were collected by filtration, and recrystallized from water. The final product was collected by filtration, washed with ethanol and then diethyl ether and finally air-dried. Chemical analyses (Found: C, 17.22%; H, 7.08%; N, 19.97%; Cr, 11.85%; Cl, 28.51%. Calculated for $C_{12}H_{60}Cl_7Cr_2N_{12}NaO_6$: C, 17.07%; H, 7.16%; N, 19.91%; Cr, 12.3%; Cl, 29.4%).

Note that $[K(OH_2)_6][Cr(en)_3]_2Cl_7$ and $[Na(OH_2)_6][Cr(en)_3]_2Br_6Cl$ were prepared as for $[Na(OH_2)_6][Cr(en)_3]_2Cl_7$ except that sodium chloride was replaced by potassium chloride and sodium bromide, respectively. Chemical analyses (Found for the first: C, 16.36%; H, 6.70; N, 19.26; Cr, 11.51%; Cl, 29.04%. Calculated for $C_{12}H_{60}Cl_7Cr_2K\ N_{12}O_6$: C, 16.74%; H, 7.02%; N, 19.54%; Cr, 12.09%; Cl, 28.85%. Found for the second: C, 13.36%; H, 5.59%; N, 15.48%; Cr, 9.23%; Br, 43.44%. Calculated for $C_{12}H_{60}Br_6ClCr_2N_{12}NaO_6$:C, 12.97%; H, 5.45%; N, 15.13%; Cr, 9.36%; Br, 43.17%.)

B. Crystallography

All crystallographic measurements were made with graphite-monochromated Mo-Kα radiation ($\lambda=0.71069$ Å) and an Enraf-Nonius CAD4 diffractometer. The data were collected in the θ-2θ mode, with

$$\Delta\theta=[0.8+0.35\tan(\theta)]^\circ$$

and a maximum scan time of 1 min.

C. Determination of the crystal structure of $[Na(OH_2)_6][Cr(en)_3]_2Br_6Cl$

Crystal data: $C_{12}H_{60}Br_6ClCr_2N_{12}NaO_6$, formula weight FW=1110.6, trigonal, $a=11.740(5)$, $c=16.008(9)$ Å; $V=1910.7$ Å^3; $Z=2$; $D_{calc}=1.93$ g cm^{-3}; F(000)=1100; μ(Mo Kα) 69.0 cm^{-1}; space group $P\bar{3}cl$.

A total of 2309 reflections were measured for $2^\circ<\theta<25^\circ$ and $+h-k+1$. There was no crystal decay. An absorbtion correction (maximum 1.26, minimum 0.70) was applied using DIFABS (Ref. 8) after isotropic refinement. After averaging symmetry related reflections ($R_{int}=0.034$), 870 unique reflections with $|F^2|>\sigma(F^2)$ were used in the final refinement, where

$$\sigma(F^2)=[\sigma^2(I)+(0.04I)^2]^{1/2}/Lp\ .$$

The structure was solved by routine heavy atom methods and refined by a full matrix least-squares method, with nonhydrogen atoms anisotropic. Hydrogen atoms were omitted. The weighting scheme was $w=\sigma^{-2}(F)$, and the final residuals were $R=0.062$ and $R'=0.068$. A final difference map was featureless. Programs from the Enraf-Nonius SDP-Plus package were run on a PDP $\frac{11}{34}$ computer.

D. Determination of the crystal structure of $[Na(OH_2)_6][Cr(en)_3]_2Cl_7$

Crystal data: $C_{12}H_{60}Cl_7Cr_2N_{12}NaO_6$, FW=843.8, trigonal, $a=11.513(2)$, $c=15.566(6)$ Å; $V=1786.7$ Å;^{3} $Z=2$; $D_{calc}=1.57$ g cm^{-3}; $F(000)=884$; μ(Mo-Kα) 11.8 cm^{-1}; space group $P\bar{3}cl$.

A total of 2349 reflections were measured for $2^\circ<\theta<25^\circ$ and $+h-k+l$. There was no crystal decay,

and no absorption correction was applied. After averaging symmetry related reflections ($R_{int}=0.030$), 799 unique reflections with $|F^2|>\sigma(F^2)$ were used in the final refinement, where

$$\sigma(F^2)=[\sigma^2(I)+(0.04I)^2]^{1/2}/Lp \ .$$

The structure is isomorphous with that of $[Na(OH_2)_6][Cr(en)_3]_2Br_6Cl$, and refinement by full matrix least squares was started from coordinates from that structure. Hydrogen atoms were located on a difference map and refined isotropically; all other atoms were anisotropic. The weighting scheme was $w=\sigma^{-2}(F)$, and the final residuals were $R=0.032$ and $R'=0.033$. A final difference map was featureless. Programs from the Enraf-Nonius SDP-Plus package were run on a Micro-Vax computer.

E. Magnetic-susceptibility measurements

The susceptibility of zero applied field was measured as earlier.[9] The crystals were oriented by microscopy. The crystals are uniaxial and the zero-field susceptibility was measured parallel and perpendicular to the unique axis; to prevent confusion, these are referred to as the longitudinal and transverse susceptibility, respectively.

F. Heat-capacity measurements

Heat-capacity measurements were performed on small crystals of $[Na(OH_2)_6][Cr(en)_3]_2Cl_7$ in the temperature region $0.08<T<0.9$ K. The calorimeter consisted of a sapphire disk with a diameter of 10 mm and a thickness of 50 μm, to which a thermometer and a heater were attached. As a thermometer we used a small piece of a thick-film resistor (Philips RC-01), whereas the heater consisted of a chromium film, evaporated on the sapphire disk. Electrical connections were made by superconducting Nb wires with a diameter of 50 μm and a length of approximately 2.5 cm. These wires were attached to a copper ring, in which the calorimeter was suspended by thin nylon wires. This ring acted as a heat sink, and was connected to the mixing chamber of a dilution refrigerator.

III. RESULTS AND DISCUSSION

A. Synthesis

Tries(1,2diaminoethane)chromium(III) chloride trihydrate, $[Cr(en)_3]Cl_3\cdot 3H_2O$, was prepared according to Gillard and Mitchell,[7] and the method was found routine and trouble free. However, all attempts to prepare the analogous bromide, $[Cr(en)_3]Br_3\cdot 3H_2O$, by the method of Rollinson and Bailar[3] were unsuccessful. Their method consists of adding solid sodium bromide to an aqueous solution of $[Cr(en)_3]Cl_3$ in a 6:1 (Na:Cr) molar ratio (described as a 100% excess of NaBr), which is purported to instantly yield crystals of the less soluble bromide analogue, reported as the tetrahydrate, $[Cr(en)_3]Br_3\cdot 4H_2O$. The product indeed analyses well for this formulation, but x-ray crystallography (*vide infra*) reveals the product to be a double salt, $[Na(OH_2)_6][Cr(en)_3]_2Br_6Cl$, a formulation which also fits the microanalytical data well. Incomplete exchange in metathetic reactions is a common phenomenon, and so this result is not too surprising, with hindsight. However, the identity of the other two salts reported by Rollinson and Bailar,[3] $[Cr(en)_3]I_3\cdot H_2O$ and $[Cr(en)_3][SCN]_3\cdot H_2O$, must now be considered unproven.

Recognition of the true nature of $[Na(OH_2)_6][Cr(en)_3]_2Br_6Cl$ allowed the preparative method to be adapted to the synthesis of both $[Na(OH_2)_6][Cr(en)_3]_2Cl_7$ and $[K(OH_2)_6][Cr(en)_3]_2Cl_7$, and clearly a much wider range of double salts could be prepared, if required.

B. Crystal structures of $[Na(OH_2)_6][Cr(en)_3]_2Br_6Cl$ and $[Na(OH_2)_6][Cr(en)_3]_2Cl_7$

The fractional atomic coordinates and principal bond lengths and bond angles for each structure are given in Table I–III. Clearly, the bond parameters in the chloride structure are much better determined than those in the mixed halide salt.

The unit cell of the mixed halide salt, $[Na(OH_2)_6][Cr(en)_3]_2Br_6Cl$, is shown in Fig. 1. The $[Na(OH_2)_6]^+$ and Cl^- ions alternate along the c axis of the crystal, with the chloride ion on a site of $\bar{3}$ symmetry, and the $[Na^+]$ cation on a site of 32 symmetry. The $[Cr]^{3+}$ cations lies on the threefold rotation axes at $x=\frac{1}{3}$, $y=\frac{2}{3}$, and $x=\frac{2}{3}$, $y=\frac{1}{3}$, and the bromide ions are in general positions. $[Na(OH_2)_6][Cr(en)_3]_2Cl_7$ shows the same site relationships, except that chloride ions, Cl(1), are found in general positions, and the unique chloride, Cl(2), is found on the c axis on a site of $\bar{3}$ symmetry.

The structure of the $[Cr(en)_3]^{3+}$ cation in these structures is unremarkable, and is very similar to that found in the structures of $[Cr(en)_3]Cl_3\cdot 3H_2O$,[5] $[Cr(en)_3]Br_3\cdot 6H_2O$,[10] and $[Cr(en)_3][Co(en)_3][SCN]_6$.[10] Of more interest is the observation of discrete hexaaquasodium(I) cations, which have only been characterized in the solid state infrequently. Thus, in trisodium fructose 1,6 diphosphate octahydrate, the two independent $[Na(OH_2)_6]^+$ cations show $\bar{r}$(NaO) at 2.41(3) and 2.42(6) Å;[11] in sodium sulfate decahydrate, the

TABLE I. Fractional atomic coordinates ($\times 10^4$) for $[Na(OH_2)_6][Cr(en)_3]Br_6Cl$ with estimated standard deviations n parentheses.

	x	y	z
Cr	3333	6667	3799(2)
N(1)	1818(7)	6566(7)	3069(5)
N(2)	2941(7)	7906(7)	4530(5)
C(1)	1691(8)	7803(9)	4241(7)
C(2)	1653(9)	7720(9)	3289(7)
Br	4875.0(10)	1042.(10)	3749.9(7)
Cl	0	0	5000
Na	0	0	2500
O	1930(8)	875(9)	3443(6)

TABLE II. Fractional atomic coordinates ($\times 10^4$) for $[Na(OH_2)_6][Cr(en)_3]_2Cl_7$ with estimated standard deviations in parentheses.

	x	y	z
Cr	3333	6667	3820.5(3)
N(1)	1795(2)	6546(2)	3080(1)
N(2)	2925(2)	7920(2)	4561(1)
C(1)	1662(2)	7816(2)	4258(1)
C(2)	1609(2)	7689(2)	3299(1)
Cl(1)	4864.7(6)	1008.2(5)	3748.7(3)
Cl(2)	0	0	5000
Na	0	0	2500
O	1984(2)	865(2)	3428(1)

two independent $[Na(OH_2)_6]^+$ cations show $\bar{r}$(NaO) at 2.43(3) and 2.43(2) Å;[12] and in sodium tetraborate decahydrate, the two independent $[Na(OH_2)_6]^+$ cations show $\bar{r}$(NaO) at 2.40(1) and 2.43(2) Å.[12] In contrast, in the slats $[Na(OH_2)_6][Cr(en)_3]_2Br_6Cl$ and $[Na(OH_2)_6][Cr(en)_3]_2Cl_7$, $\bar{r}$(NaO) is at 2.48(1) and 2.454(2) Å, respectively; the coordination geometry corresponds, as expected, to octahedral, with the bond lengths being at the upper end of the range of previously observed values $\{\bar{r}(NaO)_{lit}=2.42$ Å$\}$. The structure of

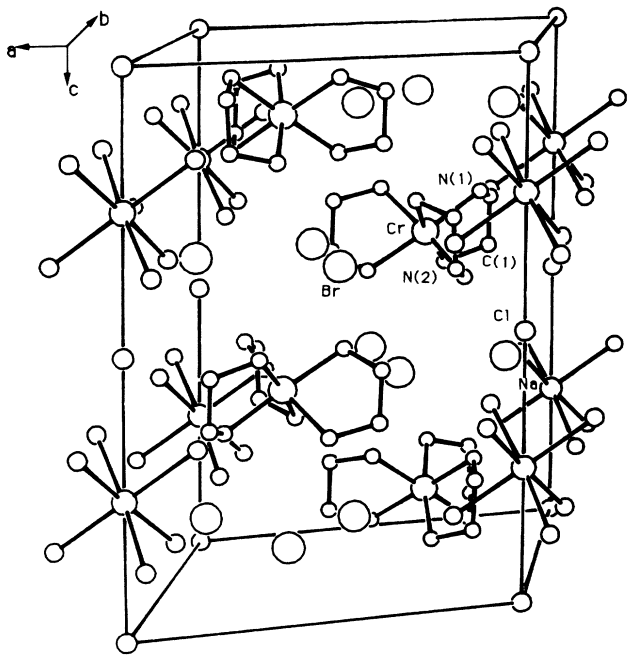

FIG. 1. The unit cell of $[Na(OH_2)_6][Cr(en)_3]_2Br_6Cl$. The hydrogen atoms are not represented.

TABLE III. Intramolecular distance (Å) and angles (°) in (I) $[Na(OH_2)_6][Cr(en)_3]_2Br_6Cl$, and (II) $[Na(OH_2)_6][Cr(en)_3]_2Cl_7$, as compared with (III) $[Cr(en)_3]Cl_3\cdot 3H_2O$, with estimated standard deviations given in parentheses. The footnotes (a)–(f) are symmetry elements.

	I	II	III (Ref. 5)
(a) Bonds			
Cr—N(1)	2.082(10)	2.059(2)	2.075(3)
Cr—N(2)	2.090(10)	2.076(2)	2.084(3)
N(1)—C(2)	1.503(16)	1.475(4)	1.463(5)
N(2)—C(1)	1.485(14)	1.475(3)	1.482(5)
C(1)—C(2)	1.526(16)	1.498(3)	1.518(5)
Na—O	2.478(9)	2.454(2)	
(b) Angles			
N(2)—Cr—N(2)[a]	91.7(3)	92.17(7)	
N(1)—Cr—N(1)[a]	91.6(3)	91.71(7)	
N(1)—Cr—N(2)[b]	171.8(3)	172.04(7)	
N(1)—Cr—N(2)	82.7(3)	82.62(8)	82.5(1)
N(1)—Cr—N(2)[a]	94.5(3)	94.03(6)	94.6(1)
N(2)—C(1)—C(2)	108.2(9)	108.5(2)	108.5(3)
Cr—N(2)—C(1)	108.7(6)	108.8(1)	108.5(2)
Cr—N(1)—C(2)	108.0(6)	108.3(1)	108.7(2)
N(1)—C(2)—C(1)	106.1(9)	107.5(2)	107.3(3)
O—Na—O[c]	86.7(3)	86.53(8)	
O—Na—O[d]	90.0(4)	88.88(7)	
O—Na—O[e]	96.7(3)	96.12(6)	
O—Na—O[f]	175.2(4)	173.14(8)	

[a] $1-y, 1+x-y, z$.
[b] $y-x, 1-x, z$.
[c] $-y, x-y, z$.
[d] $x-y, -y, \frac{1}{2}-z$.
[e] $y, x, \frac{1}{2}-z$.
[f] $-x, y-x, \frac{1}{2}-z$.

$[Na(OH_2)_6]^+$ found here appears to be the least perturbed (by hydrogen bonding) of any of those reported.

The structures of the four compounds studied here consist of trigonally distorted $[Cr(en)_3]^{3+}$ ions, with all the molecular trigonal axes parallel to the crystallographic c axis. The halide ions are relatively isolated, and connected to the (1,2 diaminoethane) groups by N—H $\cdots$ Cl hydrogen bonds. The water molecules are all found to be octahedrally coordinated to the alkali metal ions.

In order to study the superexchange interaction of the magnetic ions we have to analyze the spatial distribution of the transition-metal ions and the pathways connecting them. From the crystal symmetry and the cell dimensions of the salts, the chromium(III) cations are observed to form an almost hexagaonl closed-packed (hcp) lattice. The c dimension is contracted to a c/a ratio of close to 1.35, instead of the ideal value 1.63 for hcp, which gives each chromium(III) cation eight nearest neighbors at almost the same distance, close to 8 Å. The chromium ions are connected through hydrogen-bonded halogen ions in long superexchange paths Cr—N—H $\cdots X \cdots$ H—N—Cr, with X = Cl or Br. As a consequence of the long distances and the number of intervening atoms we expected to have a very weak magnetic exchange interaction. The water molecules do not participate in these bonds, and they form hydrogen-bonded channels by themselves, or as hexaquo alkali complexes. This independence explains the high hygroscopicity of the compounds.

C. Magnetic-susceptibility and heat-capacity results

The experimental susceptibility data are illustrated in Fig. 2 along with fitted curves to be described in the fol-

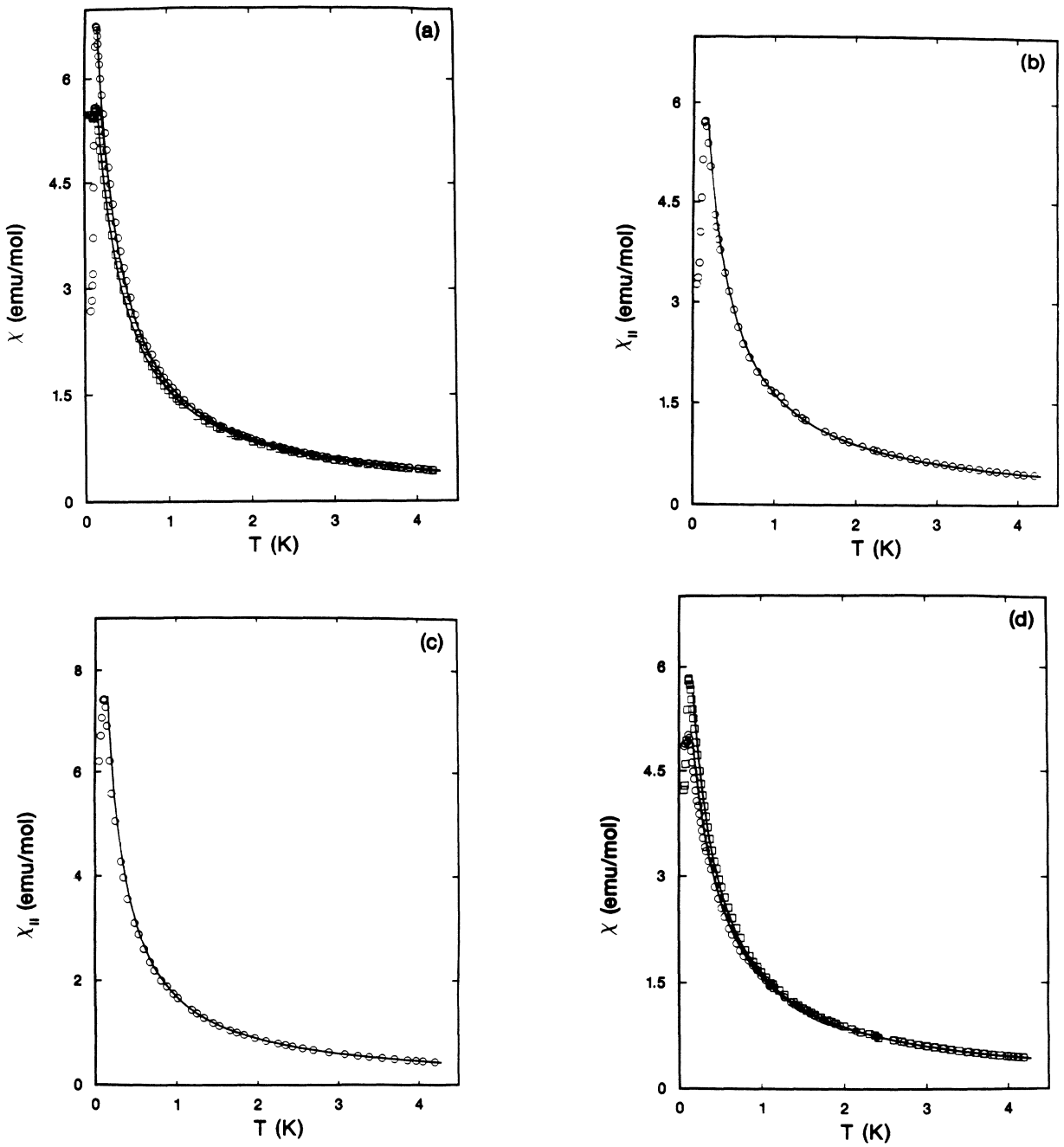

FIG. 2. The longitudinal (circles) and transverse (squares) susceptibilities of single crystals of $[Cr(en)_3]Cl_3 \cdot 3H_2O$, (a) ; $[Na(OH_2)_6][Cr(en)_3]_2Cl_7$, (b); $[K(OH_2)_6][Cr(en)_3]_2Cl_7$, (c); and $[Na(OH_2)_6][Cr(en)_3]_2Br_6Cl$, (d). The continuous lines represent the fits for exchange-corrected paramagnetism [Eqs. (1)–(3)].

lowing. It is clear from the data that all the compounds order as antiferromagnets; furthermore, no absorption was observed in the out-of-phase signal. The ordering temperatures are below 0.15 K in all the compounds as seen in Table IV, with T_c taken from the point of maximum slope in the longitudinal data sets. With such low transition temperatures, it is apparent that the exchange constant is comparable in magnitude with the zero-field splitting. Since such a situation was also found earlier[1] with $Cs_2CrCl_5 \cdot 4H_2O$, the method of analysis presented there was followed.

Generally, the heat-capacity measurements were performed by the so-called relaxation time method. Because of the increasingly large relaxation times at lower temperatures, successively smaller samples had to be used (about 10, 2, and 0.35 mg). At the lowest temperatures, we had to resort to adiabatic calorimetry. The typical error in the determination of the heat capacity amounted to 5%.

TABLE IV. Transition temperatures derived from the experimental susceptibilities, and exchange constants, zero-field splittings and Landé factors derived from the fittings of the experimental measurements to Eqs. (4) and (5).

	T_c(K)	zJ/k_B(K)	$2D/k_B$(K)	$g_\parallel$	$g_\perp$
$[Cr(en)_3]Cl_3\cdot 3H_2O$	0.124(5)	−0.061(2)	−0.091(8)	1.994	1.988
$[Na(OH_2)_6]Cr(en)_3]Cl_7$	0.116(5)	−0.068(4)	−0.058(8)	2.01	2.00
$[K(OH_2)_6][Cr(en)_3]Cl_7$	0.093(5)	−0.046(4)	−0.060(8)	1.993	1.951
$[Na(OH_2)_6][Cr(en)_3]Br_6Cl$	0.112(5)	−0.066(4)	+0.064(8)	2.001	1.991

The data were corrected for the contribution of the empty sample holder, that was measured in a separate run, and amounted to 0.5–20% of the total heat capacity. The data obtained on the various samples are plotted in Fig. 3. For clarity, the experimental heat capacity above 0.2 K, multiplied by a factor of 10, is also depicted.

The paramagnetic susceptibilities of a $^4A_2$ state with zero-field splitting $2D/k_B$ are well known[13] and are found as

$$\chi_\parallel^P=\frac{Ng_\parallel^2\mu_B^2}{4k_BT}\left[\frac{1+9\exp(-2D/k_BT)}{1+\exp(-2D/k_BT)}\right], \quad (1)$$

$$\chi_\perp^P=(Ng_\perp^2\mu_B^2/k_BT)[1+\exp(-2D/k_BT)]^{-1} +(3Ng_\perp^2\mu_B^2/4D)\tanh(D/k_BT) . \quad (2)$$

When the exchange interaction can be considered a small perturbation on the paramagnetic Hamiltonian, $|J|\ll|D|$, exchange effects may be accounted for in the usual molecular-field approximation as

$$\chi_i=\chi_i^P[1-(2zJ/Ng_i^2)\chi_i^P]^{-1} , \quad (3)$$

where $i=\parallel$ or $\perp$.

When both $|D|$ and $|J|$ are much smaller than k_BT, the linear approximations to Eqs. (1) and (2), corrected for exchange effects, are found as

$$\chi_\parallel=(Ng_\parallel^2\mu_B^2/3k_BT)\{\tfrac{15}{4}+[(\tfrac{75}{8})(zJ/k_B)-3D/k_B](1/T)\}, \quad (4)$$

$$\chi_\perp=(Ng_\perp^2\mu_B^2/3k_BT)\{\tfrac{15}{4}+[(\tfrac{75}{8})zJ/k_B+3D/2k_B](1/T)\} . \quad (5)$$

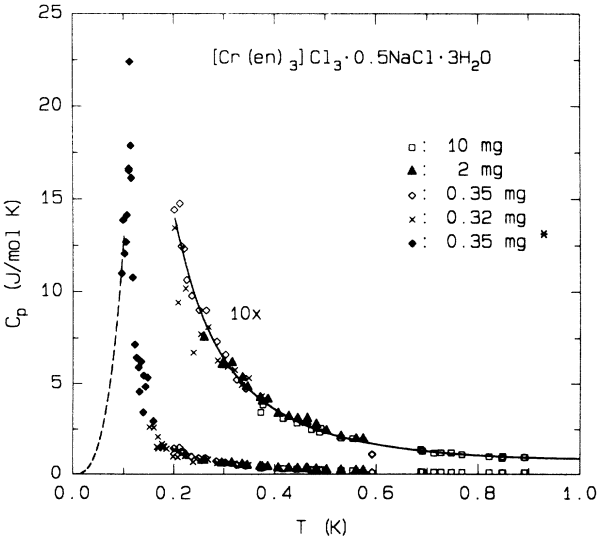

FIG. 3. Heat capacity of various samples of $[Na(OH_2)_6][Cr(en)_3]_2Cl_7$. The sample indicated by an asterisk has been measured by adiabatic calorimetry(see the text).

Note that plots of $\chi_i\cdot T$ vs $1/T$ should be linear at high temperatures. These plots for the four compounds are shown in Fig. 4. Straight lines are indeed obtained at high temperatures. The values of the parameters were obtained graphically, since the g values can be obtained from the intercepts of each of the lines, while the values of D and J may be found from the slopes of the lines. The resulting g values for $[Cr(en)_3]Cl_3\cdot 3H_2O$ are 4% lower than the experimental EPR average value, assuming the stated water content. The microanalysis of the powder suggests it to be the trihydrate, but the crystal has been grown from aqueous solution and the structure can admit additional water molecules that would account for the low values of g. Therefore, the susceptibility data for this compound has been scaled with a common factor to fit with the experimental EPR value.[6] The resulting parameters for the exchange constant zJ/k_B the zero-field splitting, $2D/k_B$ and the Landé factors, $g_\parallel$ and $g_\perp$, are given in Table IV.

The parameters agree well with the EPR results on $[Cr(en)_3]Cl_3\cdot 3H_2O$, but these measurements also yield the sign of D. The zero-field splitting is of the order of that observed in other compounds.[14] The major difference between the chloro and bromo compounds is the change in the sign of the zero-field-splitting parameter between them. This has significance for the different ordering which the two compounds undergo, as discussed in the following. The exchange constants are small and antiferromagnetic in sign.

With these parameters in hand, the data was then plotted the data over the whole temperature range along with the theoretical curves for exchange-corrected paramagnetism, Eq. (3). The only small change in the parameters which was required in order to make the best fit was found with the exchange constant for $[Na(OH_2)_6][Cr(en)_3]_2Br_6Cl$. In this case, $zJ/k_B=-0.074$ K was needed. These plots are found in Fig. 2, and it can be seen that the curves fit the experimental data quite well at temperatures down to close to the max-

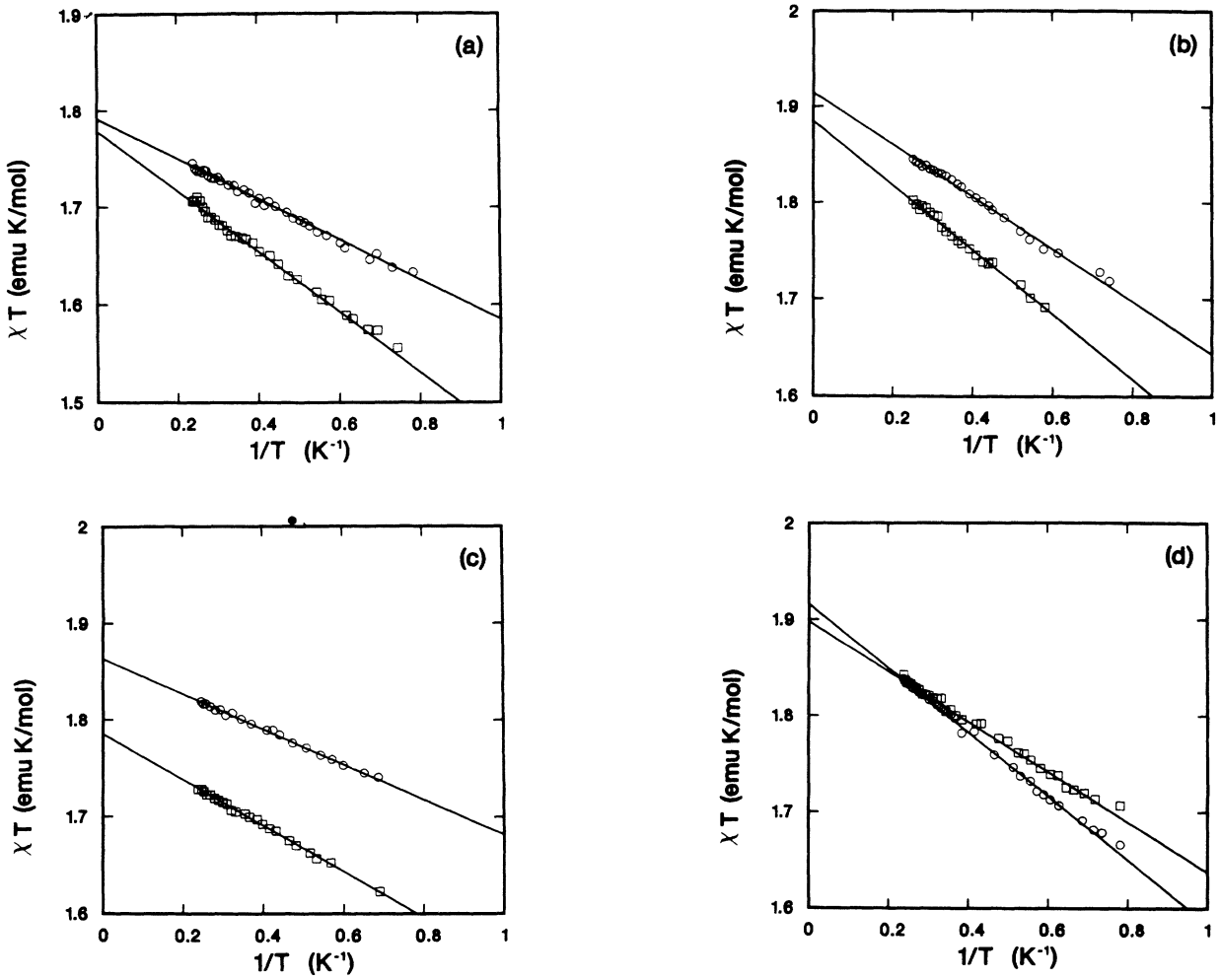

FIG. 4. Experimental susceptibilities of the four compounds above 1 K plotted as $\chi \cdot T$ vs $1/T$. Longitudinal susceptibilities are represented with circles and transverse susceptibilities with squares. The linear fits to Eqs. (4) and (5) in two directions provide the parameters as listed in Table IV. (a) $[Cr(en)_3]Cl_3 \cdot 3H_2O$; (b) $[Na(OH_2)_6][Cr(en)_3]_2Cl_7$; (c) $[K(OH_2)_6][Cr(en)_3]_2Cl_7$; (d) $[Na(OH_2)_6][Cr(en)_3]_2Br_6Cl$.

imum of the susceptibility (T_m). This kind of approach would be justified when the exchange interaction is a small perturbation on the crystal-field energy levels.

The parameters J and D are of comparable magnitude in the compounds under discussion. These terms should be introduced together in the interacting Hamiltonian and treated at a comparable level. But such a problem has not been solved and our data analysis is bounded by this limitation.

An estimation of the possible errors in the calculated values of the susceptibilities can be given by following the opposite approach. That is, one can take the exchange interaction as the dominant one, and treat the zero-field splitting as a small perturbation. In this case, we used the high-temperature series expansion prediction for a Heisenberg antiferromagnetic interaction on a bcc lattice with $S=\frac{3}{2}$ for which seven terms are known.[15] In order to improve the convergence of the series and increase the range of temperatures for which the expansion is valid, Padé approximants were applied to the direct series and to the transformed susceptibility series $(\chi)^{1/\gamma}$. The three-dimensional critical exponent $\gamma=1.405$ was taken. The susceptibility is then given by

$$\chi=\frac{Ng^2\mu_B^2 S(S+1)(P/Q)^{\gamma}}{3k_BT}\ , \tag{6}$$

where

$$P=1-56.000\,388\ \text{K}-448.0661\ \text{K}^2+2021.85165\ \text{K}^3$$

and

$$Q=1-70.235264\ \text{K}+350.76412\ \text{K}^2\ 8139.45679\ \text{K}^3 -19019.872\ \text{K}^4\ ,$$

and where $K=J/k_BT$. Finally, a first-order correction for the axial anisotropy can be applied, yielding the equations,

$$\chi_{\parallel}=\chi(1-4D/5k_BT) \tag{7}$$

$$\chi_{\perp}=\chi(1+2D/5k_BT)\ . \tag{8}$$

The value of the exchange constants can be evaluated from this analysis.

The reduced critical temperature has been located as $K_c = |J/k_B T_c| = 0.0680$, and the ratio of the ferromagnetic to the antiferromagnetic singularity is known for this model, $K_C/K_N = 1.021$. The values of the susceptibility maximum,

$$\bar{\chi}_m = \chi_m |J| / N_0 g^2 \mu_B^2 = 0.0297$$

and of the corresponding temperature

$$\tau_m = k_B T_m / |J| S(S+1) = 4.20$$

have been obtained from the Padé approximants.

From the experimental values of T_N, T_m, and χ_m averaged over the principal directions, on the cases where both directions have been measured

$$\chi_m = \tfrac{1}{3}(\chi_\parallel)_m + \tfrac{2}{3}(\chi_\perp)_m ,$$

values for zJ/k_B, -0.059 K, -0.063 K, -0.048 K, and -0.066 K, respectively, were obtained for the four compounds given in Table IV. These values agree with the values derived above from the paramagnetic analysis with zero-field splitting and weak exchange. This takes into

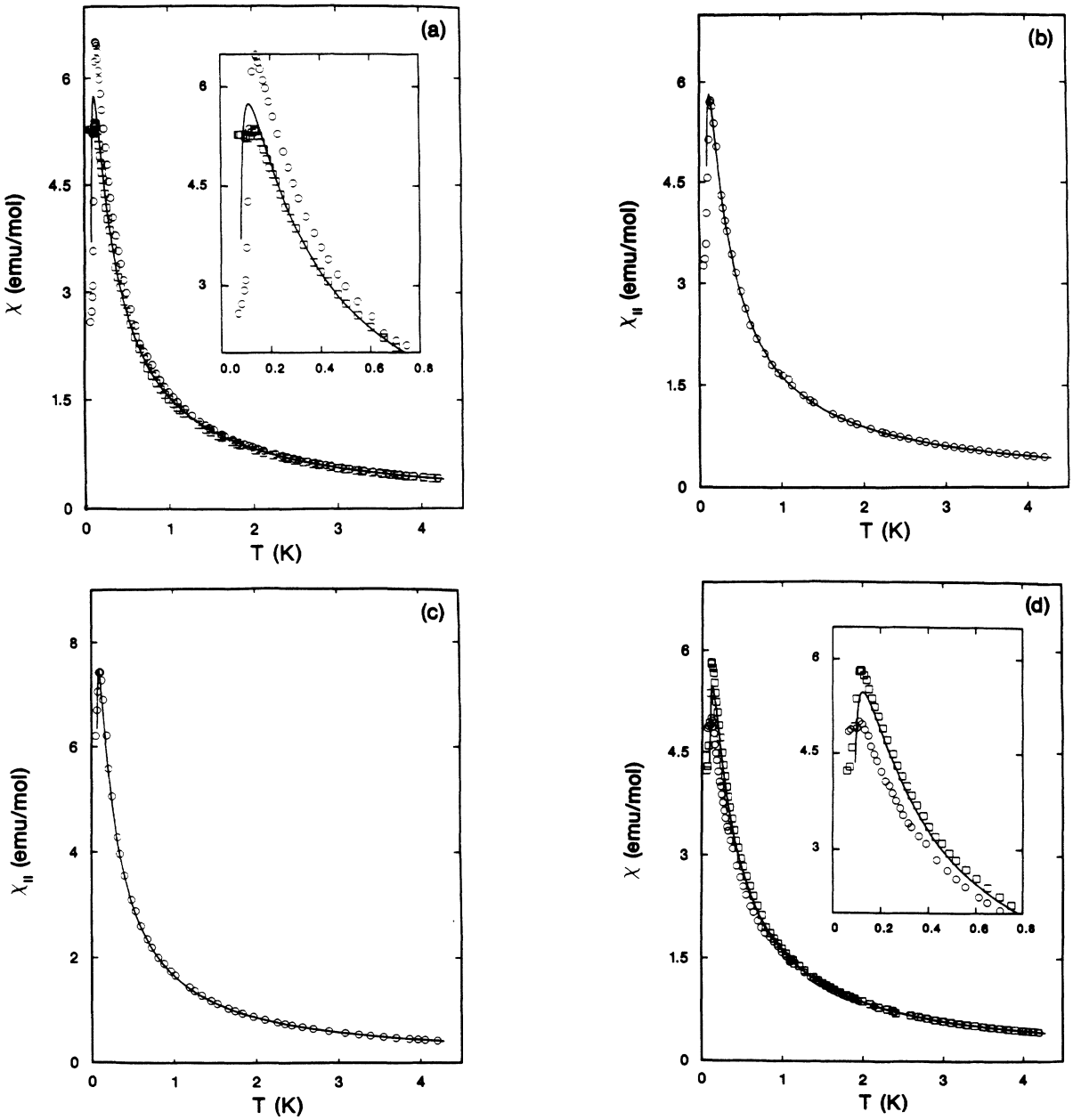

FIG. 5. Magnetic susceptibilities for a Heisenberg Hamiltonian in a bcc lattice, with $S = \frac{3}{2}$, [Eq. (6)]. The exchange parameters zJ/k_B have been calculated from the maximum of the averaged susceptibility in each compound, being -0.059 K for $[Cr(en)_3]Cl_3 \cdot 3H_2O$, (a); -0.063 K for $[Na(OH_2)_6][Cr(en)_3]_2Cl_7$, (b); -0.048 K for $[K(OH_2)_6][Cr(en)_3]_2Cl_7$, (c); and 0.066 K for $[Na(OH_2)_6][Cr(en_3)_3]_2Br_6Cl$, (d). The experimental values show the additional splitting due to single ion anisotropy, $D < 0$ in (a), and $D > 0$ in (d).

account that $z=8$ for the bcc lattice. The same g values previously derived were used. The excellent agreement between the two approaches gives us confidence in the values of the parameters reported above, and in our understanding of these systems.

Figure 5 represents the experimental measurements together with the Padé approximant calculations. The experimental susceptibility along the easy axis is expected to remain finite near $T=0$ K, as seen in the data. This effect is produced by the random occupation of the water sites. They create a randomly varying field at the nearby tris(1,2 diaminoethane)chromium(III) ions, giving rise in turn to a zero-field splitting which varies in strength and in the orientation of its principal axis.

The λ anomaly occurring in the heat-capacity measurements at 0.112 ± 0.005 K marks the onset of three-dimensional (3D) long-range order. This temperature is about 25% lower than the temperature $T_m=0.142$ K corresponding to the maximum of the susceptibility, which is not unusual for 3D antiferromagnetic (AF) systems.[16] The data in the paramagnetic region were analyzed by fitting them the expression $C=\alpha T^{-2}+\beta T^3$, where the two terms reflect the magnetic and lattice contribution, respectively. A satisfactory description of the data above 0.2 K was obtained with the parameters

$$\alpha=(57\pm1)\ \text{mJ K/mol}$$

and

$$\beta=(30\pm10)\ \text{mJ/mol}\cdot\text{K}^4\ .$$

The result of this fit is represented by the full curve in Fig. 3. Using the first term of the high-temperature series expansions, the parameter α can be expressed in the parameters of the spin Hamiltonian:

$$\alpha=R\left[\frac{D}{k_B}\right]^2+\frac{2RzJ^2S^2(S+1)^2}{3k_B^2}\ , \tag{9}$$

where R denotes the molar gas constant. If we insert the parameters $zJ/k=-0.068$ K and $2D/k_B=-0.058$ K deduced from the susceptibility measurements in this expression, we find

$$\alpha=(7\times10^{-3}+0.36/z)\ \text{J K/mol}\ .$$

For $z=6$ and 8 this yields $\alpha=67$ and 52 mJ K/mol, respectively. Comparison with the value 57 mJ K/mol obtained from the heat-capacity measurements suggests an effective number of nearest neighbors $z=8$. This value agrees with the number of nearest magnetic neighbors linked by superexchange pathways as we have analyzed for this structure. In order to estimate the entropy associated with the ordering, we have to extrapolate the heat capacity below the ordering temperature down to zero. We assumed a T^3 behavior as predicted for an isotropic AF system by linear spin-wave theory. This extrapolation is reflected by the dashed curve in Fig. 3. Integration of C/T yields a theoretical value $R\ln(2S+1)=11.52$ J/mol·K for an $S=\frac{3}{2}$ system, which is most likely due to the large uncertainty in the extrapolation below $T=0.1$ K. More than 70% of the entropy is removed below T_N, which corroborates the three-dimensional character of the present system.

Note that the easy axis of the chloro compounds lie along the longitudinal axis, as is commonly found for antiferromagnets with a small Ising or uniaxial anisotropy. This behavior is strikingly different from that of $[Na(OH_2)_6][Cr(en)_3]_2Br_6Cl$, in which the easy axis lies in the transverse plane, similar to that anticipated for a system with XY anisotropy. These different alignments of the easy axes are a consequence of the change in sign of the zero-field-splitting parameter D beween the two materials. With a $^4A_2$ single-ion ground state, an XY model magnet may be obtained when the lowest Kramers doublet is the $|\pm\frac{1}{2}\rangle$ state (D positive) and the zero-field splitting is comparable to or larger than the exchange interaction.

In a ^4F free-ion state, an octahedral crystal-field splits the orbital degeneracy in a $^4A_2$ ground-state and two excited states $^4T_2$ and $^4T_1$. The first excited state is split in an orbital singlet and a doublet by any uniaxial field, in this case a trigonal field. The introduction of spin-orbit coupling causes the ground-state spin quadruplet to split in two doublets due to the interaction with both states coming from the excited $^4T_2$ states. The ground-state quadruplet can be described by a spin Hamiltonian with $S=\frac{3}{2}$ and Landé factors

$$g_{\parallel}=2\left[1-\frac{4\lambda}{\Delta_{\parallel}}\right],\quad g_{\perp}=2\left[1-\frac{4\lambda}{\Delta_{\perp}}\right], \tag{10}$$

where $\Delta_{\parallel}$ and $\Delta_{\perp}$ are the energy differences between the ground-state orbital singlet and the excited singlet and doublet from the $^4T_2$ state, respectively. Depending whether the singlet or the doublet is lower in the excited term the resulting ground-state splitting is positive or negative according to the calculation.

$$2\text{D}=8\lambda^2\left[\frac{1}{\Delta_{\parallel}}-\frac{1}{\Delta_{\perp}}\right]. \tag{11}$$

An axial trigonal compression should produce a negative value for the splitting 2D.

In all the compounds studied here, there is a trigonal compression but additionally there is a distortion due to a small rotation between the triangles of N perpendicular to the trigonal axis that define the octahedron around the Cr^{3+} ion. Just considering a trigonal compression of a perfect octahedron we would expect a negative zero-field splitting, but the additional distortion can introduce new terms that might change the sign of the splitting.

In any case, comparing the structures analyzed in this paper, the trigonal compression is stronger in $[Na(OH_2)_6][Cr(en)_3]_2Cl_7$ than in $[Na(OH_2)_6][Cr(en)_3]_2Br_6Cl$ that would imply a more negative value of D for the chloride, as it happens. Effectively, D is negative for the first compound and positive for the second one.

The lone previous example of a three-dimensional XY antiferromagnet is the $[Co(ONC_5H_5)_6]X_2$ system, where the ligand is pyridine N oxide and X may be nitrate, perchlorate, or tetrafluoroborate.[17] These are spin $S=\frac{1}{2}$ systems, as is $Cs_2[CoCl_4]$, which is an example of the linear

chain XY antiferromagnet. For several reasons,[18] it has appeared that cobalt(II), whether in octahedral or tetrahedral stereochemistry, would be the most likely source of XY-model magnetic systems and that has proved true to date. But, octahedral chromium(III) has the same $^4A_2$ ground state as does tetrahedral cobalt(II),[13] except for the major difference that the zero-field splitting (ZFS) is much smaller. The sign of the ZFS is what determines whether a cobalt(II) sample will follow the Ising or XY model of magnetic ordering,[18] so that one requires a chromium compound with especially small exchange in order to observe the effects of the zero-field splitting on the magnetic ordering.

In this regard, it is noted that the similar compound $[Cr(NH_3)_6]Cl_3$ obeys the Curie-Weiss law in the ^{4}He temperature region with $|\theta|$ less than 0.01 K.[19] Magnetic ordering has not yet been observed in this salt, while $[Cr(NH_3)_6][ClO_4]_2Br{\cdot}CsBr$ remains paramagnetic down to 40 mK.[20]

ACKNOWLEDGMENTS

This research was supported by the Solid State Chemistry Program of the Division of Materials Research of the National Science Foundation (NSF), under Grant Nos. DMR-8211237, DMR-8515224, and DMR-8815798. The contribution by R.B. was made possible by the NSF-Spain Joint Grant No. CCB-8504-001 and the Comisión Asesora de Investigación Científica y Técnica, Project No. PB85-106. We also thank Basrah University and the Iraqi government for support (to J.A.Z.). M. Vaziri contributed to the early stages of this work, and we also thank H.D. Koppen for his assistance.

*Permanent address: Instituto de Ciencia de Materiales de Aragón, Universidad de Zaragoza–Consejo Superior de Investigaciones Científicas, 50009 Zaragoza, Spain.

[1]R. L. Carlin and R. Burriel, Phys. Rev. B **27**, 3012 (1983).
[2]R. Burriel, J. Casabó, J. Pons, D. W. Carnegie, Jr., and R. L. Carlin, Physica B **132**, 185 (1985).
[3]C. L. Rollinson and J. C. Bailar, Jr., *Inorganic Syntheses II,* edited by W. C. Fernelius (McGraw-Hill, New York, 1946), p. 196.
[4]B. N. Figgis, J. Lewis, and F. E. Mabbs, J. Chem. Soc., p. 3138 (1961).
[5]A. Whuler, C. Brouty, P. Spinat, and P. Herpin, Acta Crystallogr. B **31**, 2069 (1975).
[6]B. R. McGarvey, J. Chem. Phys. **41**, 3743 (1964).
[7]R. D. Gillard and P. R. Mitchell, *Inorganic Syntheses XIII,* edited by W. C. Fernelius (McGraw-Hill, New York, 1972), p. 184.
[8]N. Walker and D. Stuart, Acta Crystallogr. A **39**, 159 (1983).
[9]A. van der Bilt, K. O. Joung, R. L. Carlin, and L. J. de Jongh, Phys. Rev. B **22**, 1259 (1980).
[10]P. Spinat, A. Whuler, and C. Brouty, Acta Crystallogr. B **35**, 2914 (1979); **36**, 2037 (1980).
[11]N. Narendra, T. P. Seshadri, and M. A. Viswamitra, Acta Crystallogr. C **41**, 31 (1985).
[12]H. A. Levy and G. C. Lisensky, Acta Crystallogr. B **34**, 3502 (1978).
[13]R. L. Carlin, Science **227**, 1291 (1985).
[14]R. L. Carlin and R. Burriel (unpublished).
[15]P. L. Stephenson, K. Pirnie, P. J. Wood, and J. Eve, Phys. Lett. A **27**, 2 (1968).
[16]L. J. de Jongh and A. R. Miedema, Adv. Phys. **23**, 1 (1974).
[17]R. L. Carlin and L. J. de Jongh, Chem. Rev. **86**, 659 (1986).
[18]R. L. Carlin, *Magnetochemistry* (Springer-Verlag, Berlin, 1986).
[19]H. Kobayashi, T. Haseda, and M. Mori, Bull. Chem. Soc. Jpn. **38**, 1455 (1965).
[20]R. D. Chirico and R. L. Carlin, Inorg. Chem. **19**, 3031 (1980).